ULTRAVIOLET EXTINCTION PROPERTIES IN THE MILKY WAY

Lynne A. Valencic,[1,2] Geoffrey C. Clayton,[1] and Karl D. Gordon[3]
Received 2004 June 15; accepted 2004 August 5

ABSTRACT

We have assembled a homogeneous database of 417 ultraviolet (UV) extinction curves for reddened sight lines having *International Ultraviolet Explorer* spectra. We have combined these with optical and Two Micron All Sky Survey photometry, allowing estimates of the ratio of total-to-selective extinction, R_V, for the entire sample. Fitzpatrick-Massa (FM) parameters have also been found for the entire sample. This is the largest study of parameterized UV extinction curves yet published, and it covers a wide range of environments, from dense molecular clouds to the diffuse interstellar medium, with extinctions A_V ranging from 0.50 to 4.80. It is the first to extend far beyond the solar neighborhood and into the Galaxy at large, with 30 sight lines having distances greater than 5 kpc. Previously, the longest sight lines with FM parameters and R_V extended ∼1 kpc. We find that (1) the Cardelli, Clayton, & Mathis (CCM) extinction law applies for 93% of the sight lines, implying that dust processing in the Galaxy is efficient and systematic, (2) the central wavelength of the 2175 Å bump is constant, and (3) the 2175 Å bump width is dependent on environment. Only four sight lines show systematic deviations from CCM: HD 29647, 62542, 204827, and 210121. These sight lines all sample dense, molecule-rich clouds. The new extinction curves and values of R_V allow us to revise the CCM law.

Subject headings: dust, extinction — ultraviolet: general

Online material: machine-readable tables

1. INTRODUCTION

Astronomical ultraviolet (UV) studies were not possible before the advent of rocket-borne instruments and satellites because of atmospheric absorption and Rayleigh scattering. The first satellite capable of UV observations, *OAO 2*, was launched in 1968 and was followed by a host of other satellites (Cox 2000), including *Thor Delta-1* (*TD-1*), the *Astronomy Netherlands Satellite* (*ANS*), and the *International Ultraviolet Explorer* (*IUE*), among others. The data obtained by these instruments are responsible for the vast majority of contributions to studies of interstellar dust, as dust grains preferentially extinguish short-wavelength light. By comparing heavily extinguished stars against their intrinsic fluxes (the pair method), we can better understand grain properties and composition. This is important for two reasons. First, solid knowledge of grain properties will allow us to build more realistic grain models and correct for the effects of dust in stellar and galactic photometry and spectra more accurately. Second, dust grains are extremely sensitive to their environment and can yield much information about local conditions and the physical and chemical processes that affect grains.

The pair method, first used by Bless & Savage (1970), has since been used by many others to make extinction curves and study the interstellar medium (ISM) in the Milky Way (e.g., York et al. 1973; Nandy et al. 1975, 1976; Koornneef 1978; Seaton 1979; Snow & Seab 1980; Kester 1981; Meyer & Savage 1981; Aiello et al. 1982; Massa et al. 1983; Massa & Savage 1984; Savage et al. 1985; Fitzpatrick & Massa 1986, 1988, 1990, hereafter FM86, FM88, FM90, respectively;

Clayton & Fitzpatrick 1987; Aiello et al. 1988; Cardelli et al. 1988, 1989, hereafter collectively CCM; Papaj et al. 1991; Papaj & Krelowski 1992; Jenniskens & Greenberg 1993, hereafter JG93) as well as in other galaxies (Borgman et al. 1975; Nandy et al. 1981; Koornneef & Code 1981; Clayton & Martin 1985; Fitzpatrick 1985, 1986; Clayton et al. 1996; Bianchi et al. 1996; Gordon & Clayton 1998; Misselt et al. 1999; Gordon et al. 2003).

There are significant differences between dust-grain properties in the Galaxy and those found in the Small and Large Magellanic Clouds (SMC and LMC, respectively). The SMC Bar has very strong, linear FUV extinction, while the sight lines toward the LMC2 Supershell and the average LMC curve have a weaker bump and stronger FUV extinction than the average Galactic $R_V = 3.1$ curve. There are also significant differences in metallicities and gas-to-dust ratios between the Galaxy, LMC, and SMC (Bohlin et al. 1978; Gordon et al. 2003; Luck & Lambert 1992).

A major leap forward in understanding interstellar extinction occurred in 1989, when CCM suggested a mean extinction relation that depended on one parameter, the ratio of total-to-selective extinction, R_V [$=A_V/E(B-V)$]. With only very few exceptions, Galactic extinction curves tend to follow this law within the uncertainties of the calculated R_V values and the extinction curves (Fitzpatrick 1999; Clayton et al. 2000). The Galactic diffuse ISM is well described by a curve where $R_V = 3.1$; R_V can also be thought of as a rough indicator of grain size, with low-R_V sight lines having more small grains than high-R_V sight lines. The CCM extinction relation generally does not apply outside the Galaxy, although recent work has shown that there are sight lines toward the LMC that may follow CCM (Gordon et al. 2003). This law essentially replaced the Galactic average extinction curve (Seaton 1979) with a family of R_V-dependent extinction curves, with each curve representing a mean curve for sight lines of that particular value of R_V. This also showed that many of the so-called

[1] Department of Physics and Astronomy, Louisiana State University, Baton Rouge, LA 70803; valencic@phys.lsu.edu; gclayton@fenway.phys.lsu.edu.
[2] Currently at Instituto de Astronomiá, UNAM, Apartado Postal 877, Ensenada, Baja California 22800, Mexico.
[3] Steward Observatory, University of Arizona, Tucson, AZ 85721; kgordon@as.arizona.edu.

TABLE 1
COMPARISON OF PREVIOUS UV EXTINCTION STUDIES TO THE PRESENT WORK

Authorship (1)	Number of Sight Lines (2)	Instrument (3)	FM (4)	Spectral Classification (5)	R_V (6)
Savage et al. (1985).........	1415	*ANS*	No	MK	No
Aiello et al. (1988)	115	*IUE*	No	UV	No
FM90..............................	78	*IUE*	Yes	UV	No
Papaj et al. (1991)	166	*TD-1*	No	UV	No
JG93	115	*IUE*	Yes	UV	No
Barbaro et al. (2001)	252	*ANS*	Yes	MK	Yes
This work.........................	417	*IUE*	Yes	UV	Yes

anomalous sight lines (e.g., Clayton & Fitzpatrick 1987) were, in fact, normal. In addition to finding this relationship, CCM pointed out the usefulness of normalizing extinction curves to A_V, rather than $E(B - V)$, as was usually done. Compared to $E(B - V)$, A_V is a more basic quantity, and it is a direct measure of optical depth along a line of sight. Galactic extinction curves can be fitted with six parameters (FM90), which allows for quantitative analysis of extinction characteristics.

Despite all the work that has been done with extinction curves, a homogeneous database of Milky Way extinction curves does not exist. The many previous studies, listed above, used data from different instruments and variations of the pair method to construct extinction curves. Thus, the results of these studies cannot be easily compared. Also, these sight lines make up only about half of the reddened sight lines available in the *IUE* Archive. To illustrate the disparateness of previous works, Table 1 compares various aspects of previous studies to the present work. Column (1) lists authorship, column (2) lists the number of sight lines, column (3) lists the instrument the data came from, column (4) shows whether Fitzpatrick-Massa (FM) parameters were found, column (5) shows whether the extinction curves were constructed using the MK classification or UV stellar features, and column (6) shows whether IR photometry, specifically R_V, was considered for the entire sample.

In order to solve this problem, we have built a homogeneous database of over 400 extinction curves constructed in a uniform manner. Over 150 of these sight lines extend beyond 2 kpc and 30 extend beyond 5 kpc, thus sampling a much larger volume of the Galaxy than ever before. This is a much larger and more complete database than any done previously. Until the recent release of the Two Micron All Sky Survey (2MASS) database, *JHK* photometry was available for only a small fraction of the stars in the sample. Now, estimates of R_V are available for the entire sample. Thus, it is now possible to draw a

more coherent picture of extinction in the Galaxy. In the following sections we describe our database of extinction properties, present the results of our analyses, and discuss the implications for dust grains.

2. UV DATA AND EXTINCTION CURVES

For the sake of homogeneity, Hiltner's *UBV* photometry (Hiltner 1956; Hiltner & Johnson 1956) was preferred, when possible, and was obtained for 192 sight lines. In his massive compilation and assessment, Nicolet (1978) found that Hiltner's photometry was consistently of high quality. Systematic errors were typically less than 0.01 mag (Hiltner 1956), and photometry agreed well with the works of others (Nicolet 1978). Photometry in the *JHK* bands was available for all the stars in the sample from the 2MASS database (Cutri et al. 2003).

Reddened stars, observed by *IUE*, having spectral types O3 to B5 were selected for the database. An exception is HD 29647, a B8 III star, included because it has been well studied in the past (e.g., Cardelli & Savage 1988). This range of spectral types was chosen to minimize the effects of spectral mismatch in their extinction curves (Massa et al. 1983). Thorough discussions of the uncertainties in the pair method can be found in Massa et al. (1983), Savage et al. (1985), Aiello et al. (1988), and Gordon & Clayton (1998). Only "normal" stars that had good unreddened UV comparison stars were included. The lower limit on $E(B - V)$ was 0.20.

IUE spectra for all of the stars in the sample were obtained from the Multimission Archive at Space Telescope. The archive spectra were reduced using NEWSIPS and then recalibrated using the method developed by Massa & Fitzpatrick (2000). The signal-to-noise ratios of the NEWSIPS *IUE* spectra have been improved by 10%–50% over those of IUESIPS *IUE* spectra (Nichols & Linsky 1996). Low-dispersion LWR/LWP and SWP spectra were selected from either aperture. Multiple

TABLE 2
PHOTOMETRY AND SOURCES USED IN PRESENT WORK

Name	Spectral Type	UV Type	U	B	V	J	H	K	*UBV* Source	*U* Source[a]	Non-2MASS Source
HD 14052	B1 Ib	B1 Iab	7.90 ± 0.01	8.48 ± 0.01	8.18 ± 0.01	7.51 ± 0.03	7.50 ± 0.03	7.42 ± 0.02	1	...	...
HD 14357	B2 II	B2 Ib	8.31 ± 0.01	8.83 ± 0.01	8.52 ± 0.01	7.86 ± 0.03	7.83 ± 0.02	7.80 ± 0.02	1	...	...
HD 41690	B1 V	B1.5 III	7.31 ± 0.01	7.93 ± 0.01	7.71 ± 0.01	7.20 ± 0.02	7.23 ± 0.02	7.20 ± 0.03	1	...	...
HD 199216	B1 II	B2 III	7.05 ± 0.01	7.51 ± 0.01	7.03 ± 0.01	6.05 ± 0.02	6.03 ± 0.03	5.97 ± 0.02	1	...	...
HD 203938	B0.5 IV	B1.5 III	7.13 ± 0.01	7.54 ± 0.01	7.08 ± 0.01	5.97 ± 0.02	5.88 ± 0.02	5.81 ± 0.02	1, 2	...	...
HD 235783	B1 Ib	B1 Iab	8.14 ± 0.01	8.85 ± 0.01	8.68 ± 0.01	8.28 ± 0.03	8.27 ± 0.05	8.26 ± 0.02	1	...	...

NOTE.—Table 2 is published in its entirety in the electronic edition of the *Astrophysical Journal*. A portion is shown here for guidance regarding its form and content.

[a] If not the same as *UBV* Source.

TABLE 3
PHOTOMETRY SOURCES

Number	Citation
1.................................	Hiltner (1956)
2.................................	Nicolet (1978)
3.................................	Schild et al. (1983)
4.................................	Haupt & Schroll (1974)
5.................................	Guetter (1974)

NOTE.—Table 3 is published in its entirety in the electronic edition of the *Astrophysical Journal*. A portion is shown here for guidance regarding its form and content.

spectra from one camera were averaged, and then the long- and short-wavelength segments were merged at the shortest wavelength of the SWP. The wavelength coverage is ∼1200–3200 Å with a resolution of ∼5 Å.

The standard pair method, in which a reddened star is compared with an unreddened one of the same spectral type, was used to construct each sight line's extinction curve (Massa et al. 1983). The comparison stars were selected from Cardelli et al. (1992) and dereddened. The spectral matches were made by comparing the UV spectra of pairs of stars rather than matching their visible spectral types. Here R_V was estimated from the *JHK* colors as described in Fitzpatrick (1999), and A_V was found using R_V and $E(B - V)$. In general, our UV spectral classifications are in good agreement with those that have been published previously (e.g., Aiello et al. 1988; Clayton & Fitzpatrick 1987; Papaj et al. 1991). Photometry, sources, MK and UV spectral types, reddenings, and calculated R_V values for all sight lines can be found in Tables 2, 3, and 4.

The resulting extinction curves were fitted with the FM parameterization (FM90) and then normalized to A_V. Setting $x = 1/\lambda$, the FM fitting function is given by

$$k(x) = \frac{E(\lambda - V)}{E(B - V)} = c_1 + c_2 x + c_3 D(x, \gamma, x_0) + c_4 F(x), \quad (1)$$

where

$$D(x, \gamma, x_0) = \frac{x^2}{(x^2 - x_0^2)^2 + (x\gamma)^2} \quad (2)$$

and for $x \geq 5.9 \ \mu m^{-1}$,

$$F(x) = 0.5392(x - 5.9)^2 + 0.05644(x - 5.9)^3, \quad (3)$$

while $F(x) = 0$ for $x < 5.9 \ \mu m^{-1}$.

Equation (1) results in six parameters, c_1, c_2, c_3, c_4, x_0, and γ, each of which describe different attributes of the curves. The first two, c_1 and c_2, account for the intercept and slope of the linear background. They are not independent of each other and can be merged into one parameter (Carnochan 1986; FM88), although that is not done here. The quantities c_3 and c_4 correspond to the strength of the bump and the curvature of the FUV rise. The last two parameters, x_0 and γ, correspond to the central wavenumber and width of the bump, respectively; x_0 does not vary greatly from sight line to sight line, so it may be possible to reduce the number of parameters to four overall (Fitzpatrick 1999). As can be seen in equations (2) and (3), the bump is fitted by a Drude profile, and the FUV extinction is fitted by a nonlinear function. The parameters were found using the three-step method of Gordon et al. (2003) over the wavelength range 2700–1250 Å. The FM fit is not reliable longward of 2700 Å (E. Fitzpatrick 2002, private communication). The spectra are cut at the blue end at 1250 Å in order to exclude the Lyα feature at 1215 Å. The normalization of the FM parameters was converted from $E(B - V)$ to A_V (JG93):

$$\frac{A(\lambda)}{A(V)} = \frac{k(x)}{R_V} + 1.0$$

so that the FM parameters become

$$c_1^{A_V} = c_1/R_V + 1.0,$$
$$c_j^{A_V} = c_j/R_V, \ j = 2, \ 3, \ 4.$$

The resulting normalized FM parameters are listed in Table 5. The dust environment was assessed by considering the traditional density measure, A_V/d; JG93 found that sight lines passing through dense regions had $A_V/d > 0.9$ mag kpc^{-1}, while more diffuse sight lines had $A_V/d < 0.9$ mag kpc^{-1}. We have adopted this criterion for this study. This parameter can be inaccurate since the density is averaged over the entire sight line (JG93). Other groups have noted that trends in extinction characteristics, especially those associated with the bump, can be linked to environmental influences (FM86; Cardelli & Clayton 1991; JG93).

Figure 1 shows the distribution of previously published sight lines in the Galaxy with FM parameters normalized to $E(B - V)$ and the sight lines in this new database. Because of our much larger sample, we have more complete coverage of nearby associations and more distant sight lines than previous works pushing out farther into the Galaxy and sampling a wider variety of environments. As distances were estimated using

TABLE 4
GENERAL EXTINCTION CHARACTERISTICS

Name	$E(B - V)$	R_V	A_V	Distance (pc)	Max. Distance (pc)	Min. Distance (pc)
HD 14052	0.49 ± 0.04	2.99 ± 0.19	1.47 ± 0.14	4195.08	3322.81	6065.88
HD 14357	0.48 ± 0.04	2.90 ± 0.21	1.39 ± 0.15	3817.16	2838.24	5229.96
HD 41690	0.47 ± 0.04	2.91 ± 0.22	1.37 ± 0.16	820.92	602.25	1111.31
HD 199216	0.72 ± 0.04	2.62 ± 0.36	1.88 ± 0.27	1567.69	1155.49	2380.10
HD 203938	0.71 ± 0.04	3.13 ± 0.14	2.22 ± 0.16	496.81	362.62	672.56

NOTE.—Table 4 is published in its entirety in the electronic edition of the *Astrophysical Journal*. A portion is shown here for guidance regarding its form and content.

TABLE 5

FM PARAMETERS

Name	$c_1/R_V + 1.0$	c_2/R_V	c_3/R_V	c_4/R_V	x_0	γ
HD 14052	1.1856 ± 0.3918	0.2271 ± 0.0258	0.8595 ± 0.1237	0.2124 ± 0.0411	4.5740 ± 0.0140	0.8440 ± 0.0280
HD 14357	1.1134 ± 0.1461	0.2745 ± 0.0282	1.0155 ± 0.1364	0.2421 ± 0.0296	4.5830 ± 0.0050	0.8970 ± 0.0280
HD 41690	1.3412 ± 0.2734	0.2326 ± 0.0347	0.7100 ± 0.1193	0.2790 ± 0.0494	4.6050 ± 0.0120	0.7800 ± 0.0270
HD 199216	0.7992 ± 0.2038	0.2908 ± 0.0436	1.3424 ± 0.2244	0.1408 ± 0.0339	4.5900 ± 0.0090	0.9360 ± 0.0340
HD 203938	1.1581 ± 0.3085	0.1933 ± 0.0190	1.1735 ± 0.1534	0.1371 ± 0.0217	4.5580 ± 0.0110	1.0120 ± 0.0340

NOTE.—Table 5 is published in its entirety in the electronic edition of the *Astrophysical Journal*. A portion is shown here for guidance regarding its form and content.

spectroscopic parallaxes, the uncertainties for stars plotted in Figure 1 are large, with an average uncertainty of 50%.

3. DISCUSSION

3.1. *Continuum Extinction*

The relationships between the various FM parameters were investigated, as well as their dependence on R_V^{-1}. These are shown in Figures 2–8. For pairs of parameters with significant correlations, best-fit lines are plotted using the least absolute deviation method, as this is less affected by outliers than χ^2 minimization.

There is a clear correlation between $c_1/R_V + 1.0$ and c_2/R_V (see Table 6 and Fig. 2). This has been noted before (Carnochan 1986; FM86; JG93). According to FM88, $c_1 = -3.00c_2 + 2.04$, while JG93 find that $c_1 = (-3.11 \pm 0.11)c_2 + (2.14 \pm 0.07)$. This relation shows how tightly constrained the linear component of the extinction is with respect to x (FM88). There is also a weak correlation between c_2/R_V and c_3/R_V. Neither JG93 nor FM88 found any apparent relationships between the parameters c_2 and c_3. Similarly, no correlation was found in our sample between these parameters. A comparison of the parameters found in this study and those of JG93 and FM88 are shown in Figure 3. The values of c_2 and c_3 from the other groups have been divided by the values of R_V found in this work, and the best-fit line in the lower panel was found by considering points from both studies. It was similar to that found here: $c_3/R_V = 1.77c_2/R_V + 0.67$ versus $c_3/R_V = 1.75c_2/R_V + 0.54$. As both c_2/R_V and c_3/R_V increase with R_V^{-1} and thus are influenced by similar environmental effects, perhaps it is not surprising that they themselves are correlated with each other.

The parameters c_4/R_V and c_2/R_V do not show a correlation; neither do the parameters c_2/R_V and γ. These agree with the findings of FM88 and JG93. There is also no correlation ($r = 0.13$) between c_4/R_V and γ. This is in disagreement with the findings of Carnochan (1986), FM88, and JG93, of whom the latter found a correlation coefficient $r = 0.33$ for these parameters. These groups suggested that wider bumps tended to be found along sight lines with steep FUV rises, although this correlation was weak. In the present sample, there was no correlation, regardless of whether the parameter c_4 was normalized to $E(B - V)$ or A_V. This reinforces the idea that factors influencing the bump width are distinct from those influencing the carrier of the FUV rise (FM88).

Correlations between c_2, c_3, c_4, and R_V^{-1}, noted by CCM, are confirmed here, as is the absence of a correlation between x_0
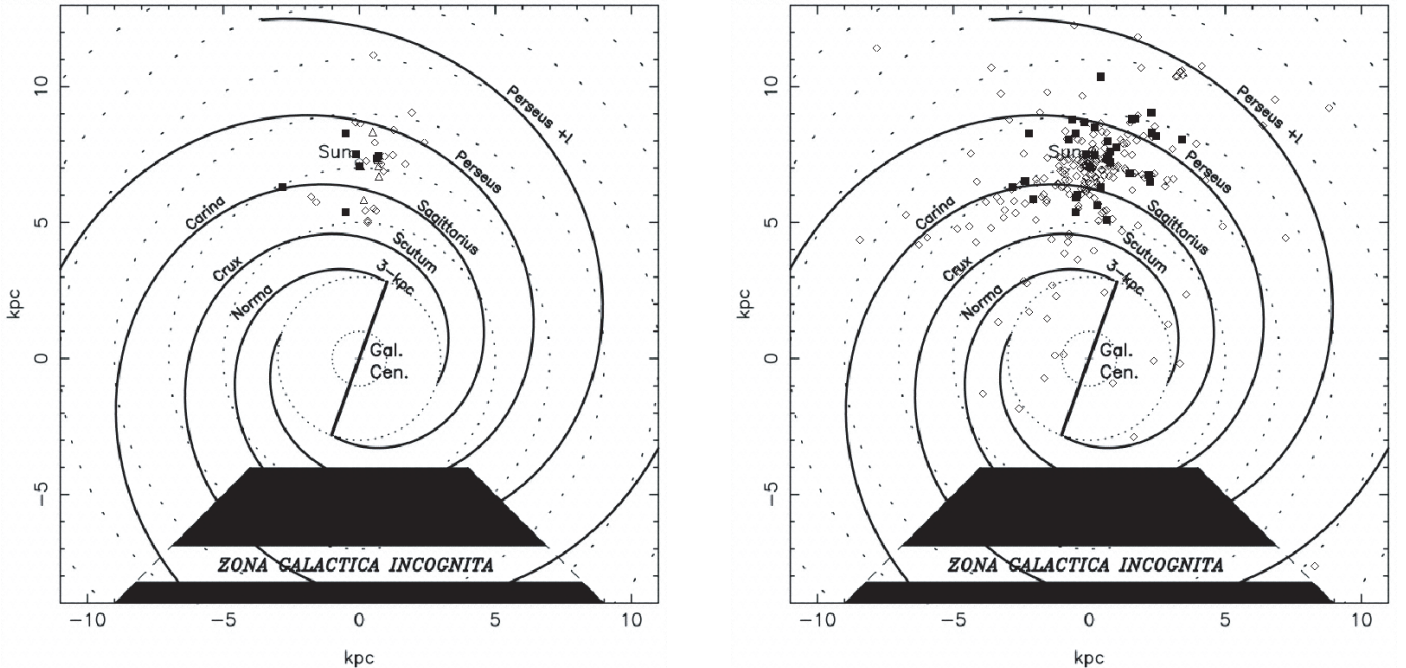

FIG. 1.—*Top*: All sight lines with published FM parameters. *Diamonds*: Aiello et al. (1988); *triangles*: FM90; *squares*: OB associations with at least one member having FM parameters. *Bottom*: All sight lines in the database. *Diamonds*: field stars; *squares*: OB associations with at least one member having FM parameters. The Galaxy overlay is from Vallée (2002).
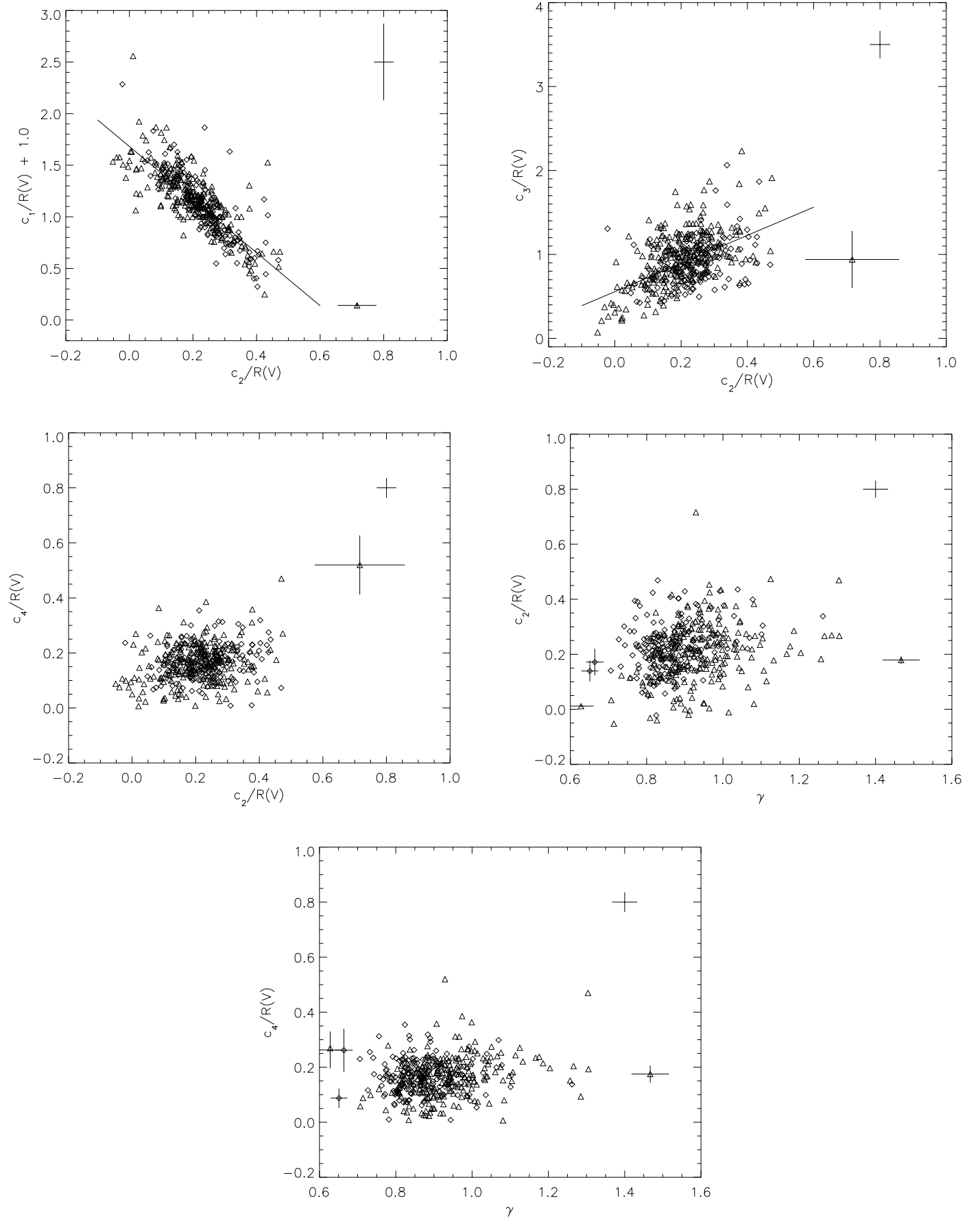
FIG. 2.—FM parameters of database sight lines. All parameters except x_0 and γ have been divided by R_V and thus normalized to A_V. Dense sight lines (those with $A_V/d \geq 0.9$ mag kpc^{-1}) are indicated by triangles, while diffuse sight lines ($A_V/d < 0.9$ mag kpc^{-1}) are indicated with diamonds. Representative error bars are indicated.

r	Absolute Deviation	Linear Fit
0.58............................	0.19	$c_3 = 2.12\gamma - 0.95$
−0.79	0.13	$c_1 = -2.54c_2 + 1.67$
0.49............................	0.54	$c_3 = 1.75c_2 + 0.54$

and R_V^{-1}. Also, while γ shows real variation, it does not appear to be linked with R_V^{-1}. These can be seen in Figure 4.

3.2. *The 2175 Å Bump*

As the 2175 Å bump is the only spectral feature yet known in the UV, the parameters that describe it were carefully considered. In Figure 5 a relationship between c_3/R_V and γ, very similar to the well-known relationship between c_3 and γ, can be seen. The values of c_3/R_V are more confined at lower γ, but as γ increases, c_3/R_V widens its range, with a general trend to increase with γ. This was noted by both FM88 and JG93 in their studies of c_3 and γ; JG93 attributed it to the fitting procedure, but FM88 suggested that these two parameters are truly related in some way.

The width of the bump shows real variation and environmental dependence. Values for γ ranged from $0.63 \pm 0.03\ \mu\mathrm{m}^{-1}$ (HD 24263) to $1.47 \pm 0.05\ \mu\mathrm{m}^{-1}$ (HD 29647). This is a wider range than that reported by FM86 [$\gamma = (0.77 \pm 0.09) - (1.25 \pm 0.07)\ \mu\mathrm{m}^{-1}$], perhaps reflecting the larger volume of the Galaxy and wider range of environments covered by this study. The average value in our sample is $\gamma = 0.92 \pm 0.12\ \mu\mathrm{m}^{-1}$. HD 29647 and HD 62542 have the broadest bumps, with $\gamma = 1.467 \pm 0.049\ \mu\mathrm{m}^{-1}$ and $\gamma = 1.304 \pm 0.04\ \mu\mathrm{m}^{-1}$, respectively. The average γ for dense and diffuse sight lines as defined above does not differ significantly, as $\gamma_{\mathrm{dense}}^{\mathrm{avg}} = 0.95 \pm 0.04\ \mu\mathrm{m}^{-1}$ and $\gamma_{\mathrm{diffuse}}^{\mathrm{avg}} = 0.87 \pm 0.03\ \mu\mathrm{m}^{-1}$. This likely reflects the density parameter's inability to sort out high versus low densities over long distances, as discussed previously. A z-test (i.e., Naiman et al. 1983) was done on the diffuse and dense γ subsets. A z-test is essentially the same as a t-test, as it is used to determine if two different data sets have significantly different mean values, but is used for large samples. As with the t-test, the resulting significance of such a test ranges from 0 (the samples have significantly different means) to 1 (the samples have essentially the same means). For example, a significance of a few hundredths indicates that two samples have significantly different means. For the dense and diffuse sight lines, the resulting significance was $\sim 10^{-6}$, which implies that there is a very significant difference between the mean γ-values of the dense and diffuse subsets. Figure 6 shows a plot of all of the sight lines and their environmental dependence and a plot of sight lines that are more than 3 σ from the mean value of γ. It can be seen that there is a clear trend that the narrowest bumps tend to be found along sight lines with $A_V/d < 0.9$ mag kpc^{-1}, the "diffuse" subset. These results strengthen those of FM86 and Cardelli & Clayton (1991), who found that lines of sight that passed through bright nebulosities (diffuse sight lines) had narrower bumps than those that passed through dark clouds.

Figure 7 compares $c_4/R(V)$ and $c_3/R(V)$, with respect to γ. It can be seen that as the bump height increases, the range of values of the FUV rise increases, and the sight lines with the widest bumps tend to have higher values of $c_3/R(V)$, all of which has been reported previously by FM88. This is likely a reflection of the dependence of $c_3/R(V)$ and γ on R_V^{-1}. No
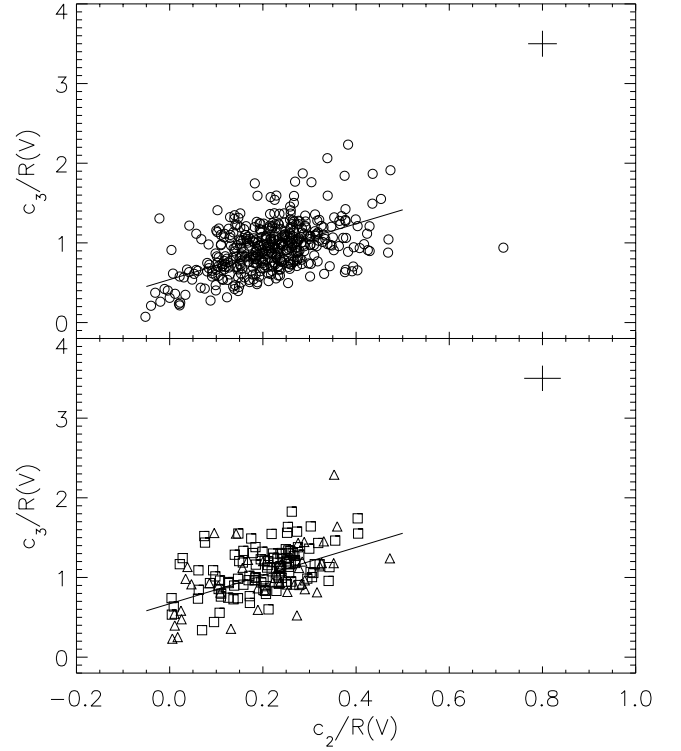

FIG. 3.—*Top*: FM parameters c_2 and c_3 from all database sight lines, divided by R_V and thus normalized to A_V. *Bottom*: Values of c_2 and c_3 from FM88 (*triangles*) and JG93 (*squares*), divided by R_V and thus normalized to A_V. Representative error bars are indicated in both panels.

similar trends can be seen between $c_4/R(V)$ and γ, as was discussed earlier.

Figure 8 plots γ versus x_0, the bump central wavelength, for the sample. This figure shows that while γ varies significantly from one sight line to another, x_0 does not. The extremely narrow range of x_0 agrees with FM86, who found that the mean $x_0 = 4.60\ \mu\mathrm{m}^{-1}$. They find extreme values of x_0 are within $\pm 0.04\ \mu\mathrm{m}^{-1}$ of the mean. Neither HD 62542 nor HD 29647 were included in the FM86 sample. JG93 found a similar value of $\langle x_0 \rangle = 4.58 \pm 0.01\ \mu\mathrm{m}^{-1}$ for the Aiello et al. (1988) sample. For the much larger sample studied here, $\langle x_0 \rangle = 4.59 \pm 0.01\ \mu\mathrm{m}^{-1}$, with values ranging from $4.50 \pm 0.04\ \mu\mathrm{m}^{-1}$ (HD 145792) to $4.70 \pm 0.03\ \mu\mathrm{m}^{-1}$ (HD 29647).

With the possible exception of HD 29647, it appears that x_0 does not vary from sight line to sight line. Cardelli & Savage (1988) found that the 2175 Å bumps toward both HD 62542 and HD 29647 were significantly shifted to shorter wavelengths. However, we find $x_0 = 4.54 \pm 0.03\ \mu\mathrm{m}^{-1}$ for HD 62542. Cardelli & Savage (1988) found $x_0 = 4.74 \pm 0.03\ \mu\mathrm{m}^{-1}$, and in the extinction curve shown in their work, the bump is visibly shifted blueward. In an effort to reproduce their results, the same *IUE* spectra and UV comparison star were used to construct an extinction curve. This curve was then fitted over three ranges: the original FM90 range (3.3–8.7 $\mu\mathrm{m}^{-1}$), from 3.7 to 8.0 $\mu\mathrm{m}^{-1}$, and from 3.7 to 8.7 $\mu\mathrm{m}^{-1}$ excluding the region around Lyα. None of these ranges produced a shifted bump. While the spectra used by Cardelli & Savage (1988) are the same as those used here, their spectra were reduced and calibrated with a different software package than those in the final archive.

In our sample of 417 sight lines, only one was shifted as much as 3 σ beyond the mean. We find $x_0 = 4.70 \pm 0.03\ \mu\mathrm{m}^{-1}$
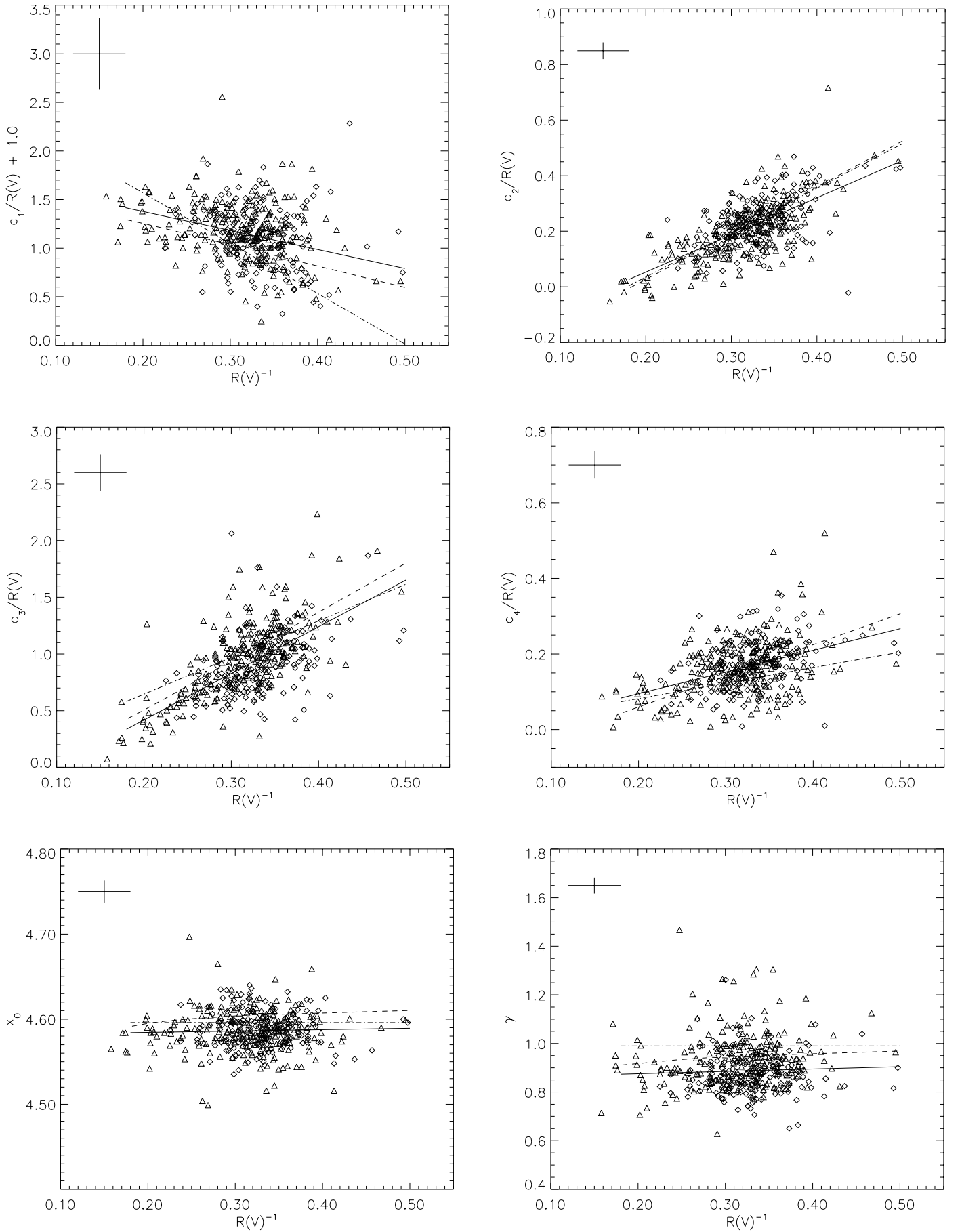
Fig. 4.—FM parameters plotted against R_V^{-1}. All parameters except x_0 and γ have been divided by R_V and thus normalized to A_V. Symbols are the same as defined in Fig. 2. The solid lines represent the best fits. The dashed lines indicate the expected values from the CCM relation; the dash-dotted lines are from the Fitzpatrick (1999) reformulation of the CCM law. Representative error bars are indicated.
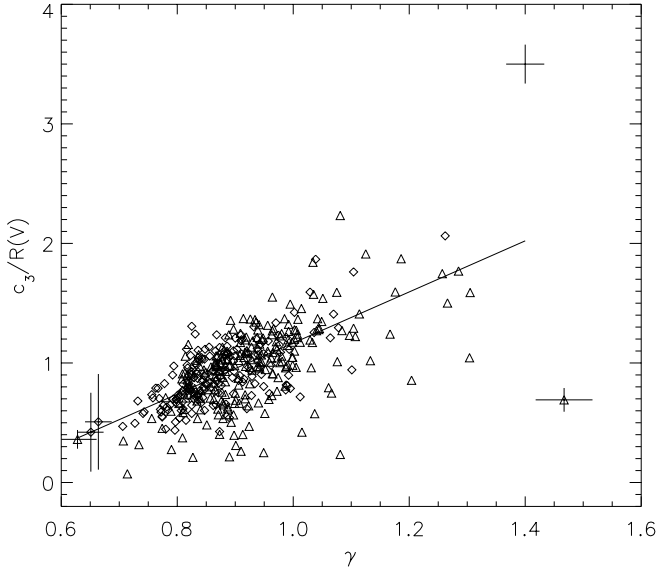
FIG. 5.—Bump height, c_3, vs. bump width, γ. Symbols are the same as defined in Fig. 2. Representative error bars are indicated.

FIG. 7.—FUV curvature, c_4/R_V, vs. bump height, c_3/R_V. Symbols are the same as defined in Fig. 2. Representative error bars are indicated. The bump height and FUV curvature are plotted with respect to bump width. Values of γ were split into three categories, each roughly pertaining to environment, with diamonds indicating $\gamma < 0.9$, triangles indicating $0.9 < \gamma < 1.1$, and squares indicating $\gamma > 1.1$.

for HD 29647, the same value found by Cardelli & Savage (1988). The other two fitting ranges that were considered when testing for HD 62542's bump shift were applied to HD 29647. The values of x_0 that were found were within 1 σ of the mean. Thus, it is quite possible that the shift in the HD 29647 bump is also fit-dependent. Another sight line, lying close to that of HD 29647, has been studied (Clayton et al. 2003). Both sight lines pass through the Taurus Dark Cloud. The second sight line, toward HD 283809, shows no evidence of a shifted bump.

If the carrier is small graphite grains, then $\gamma \propto 1/a$, where a is the grain radius, while x_0 is not a function of size (Bohren & Huffman 1983; Hecht 1986). Hecht concluded that some fraction of small ($a < 50\,\text{Å}$) carbonaceous grains are bare, and these are responsible for the bump. In this scenario, the bump width is dependent on the temperature and size distribution of these grains. The remaining small carbon grains are hydrogenated,
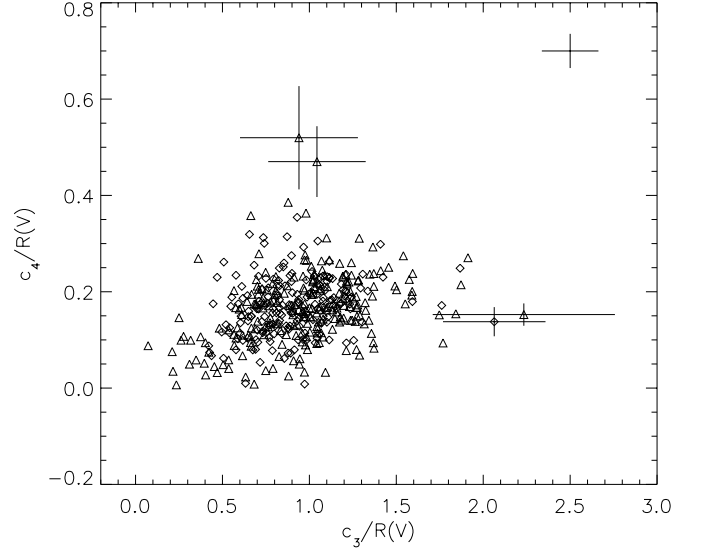
which would suppress the bump (Hecht 1986). One drawback to this model was that it required an overabundance of small grains in dense regions relative to diffuse regions (FM86; Sorrell 1990), since a large value of γ implies small grain size in this scenario. This conflicts with the observation that dense regions tend to have higher values of R_V, indicating the prevalence of large grains. However, since x_0 is not dependent on R_V (or anything else), the grains that produce the bump may form a separate population from those that are responsible for variations in R_V (CCM). On the other hand, it can be seen in Figure 4 that there is a weak correlation between γ and R_V^{-1}. This agrees with the finding that γ is environment-dependent. In 1990, Sorrell expanded on the work of Hecht (1986), suggesting that the accretion of hydrogen on larger graphite grains with
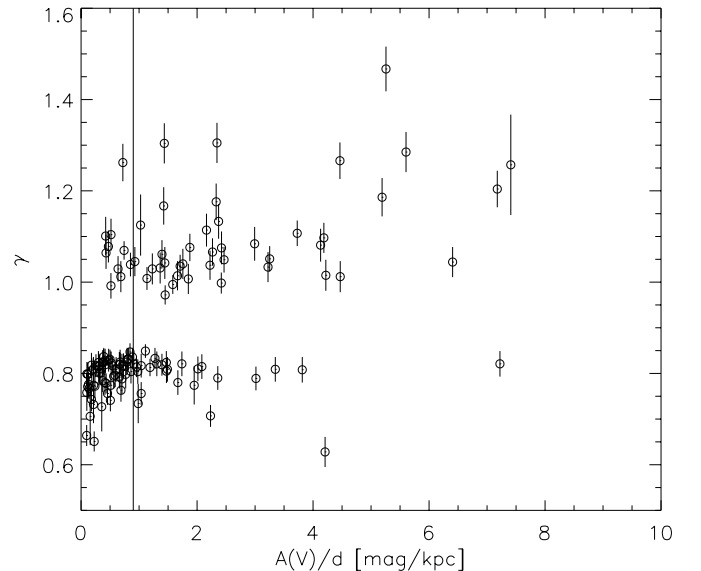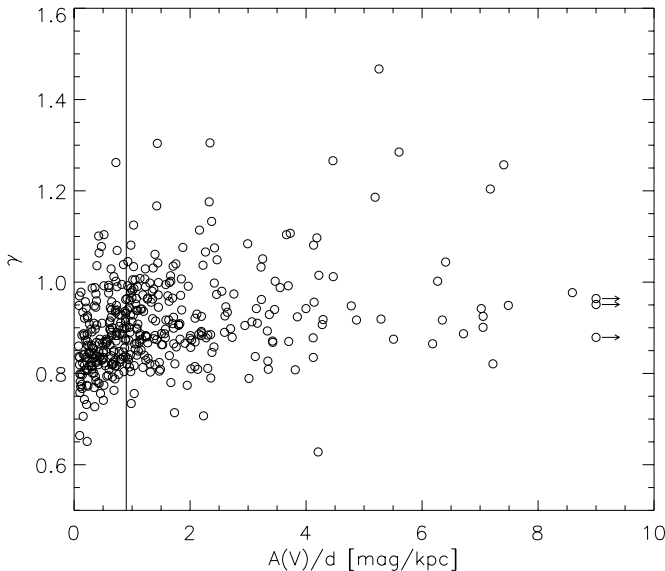

FIG. 6.—Bump width, γ, vs. density. In both, the solid line at $A_V/d = 0.9$ indicates the cutoff between dense and diffuse lines of sight. *Left*: All sight lines in database. *Right*: Sight lines beyond 3 σ of the mean. In order to make the correlation easier to see, those lines of sight that agreed with the mean were removed; the remainder are shown in the right hand panel.
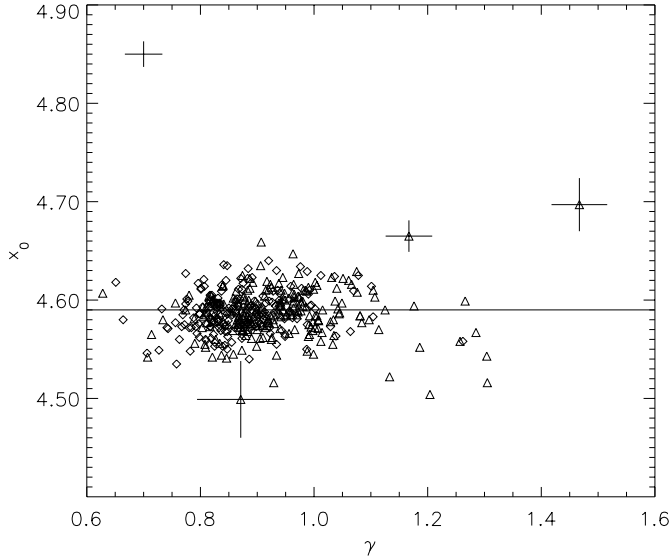
Fig. 8.—Bump central wavelength, x_0, vs. bump width, γ. The solid line represents the average. Symbols are the same as defined in Fig. 2. Representative error bars are indicated.
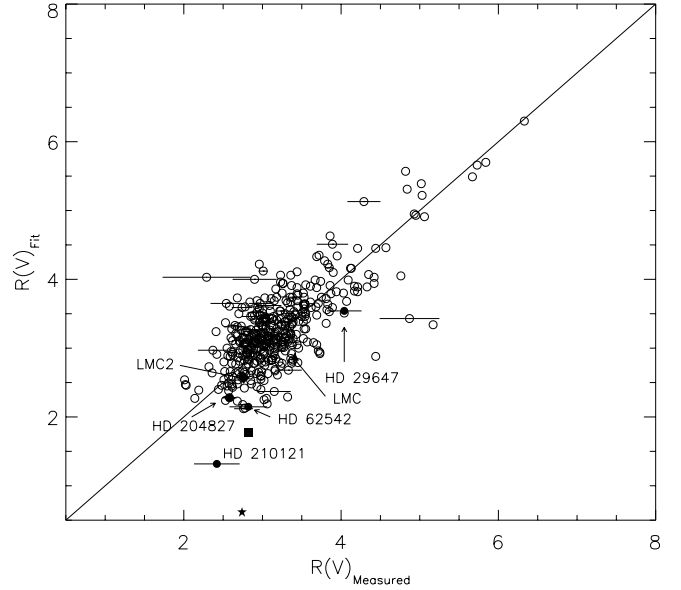

Fig. 9.—Best-fit R_V values, found through χ^2 minimization, compared to R_V values found through IR photometry. A line of slope unity has been overlaid. Four lines of sight with unusual extinction are indicated (*filled circles*). Lines of sight where the best-fit R_V did not agree with the measured value are indicated with error bars. The average LMC (*filled triangle*), LMC2 Supershell (*filled diamond*), and SMC (*filled star*) are plotted. From Clayton et al. (2000), the average low-density sight line for a Galactic region with extinction similar to that of the Magellanic Clouds (the "SD region") is also shown (*filled square*).

60 Å $< a < 80$ Å was responsible for the variations in γ. He suggested that hydrogenation of grains in dense regions broadens the bump, without affecting x_0.

Mathis (1994) considered diamond, amorphous carbon (AMC), water ice, and polycyclic aromatic hydrocarbon (PAH) mantles on graphite cores. He found that the diamond coating tended to shift x_0 to much longer wavelengths. A thin coating of AMC yields $x_0 = 4.57 \ \mu m^{-1}$ but produces a low $\gamma = 0.84 \ \mu m^{-1}$. Increasing the thickness of the mantle does not increase γ to values that are observed; a thicker mantle only broadens the bump to $\gamma = 0.93 \ \mu m^{-1}$. Hydrogenated AMC mantles are even less suitable, as they shift x_0 to longer wavelengths while having even less of an impact on γ than AMC did. Water-ice mantles may broaden γ, but only one sight line in our sample (HD 29647) has the telltale 3.07 μm ice feature (Goebel 1983). Warren (1984) showed that ice mantles do not affect the bump because there is almost no absorption at wavelengths near 2175 Å. Neutral PAHs are also possible bump-grain candidates, as they can produce both x_0 and γ consistent with observations, with $x_0 \approx 4.61 \ \mu m^{-1}$ for $\gamma = 1.0 \ \mu m^{-1}$ (Mathis 1994). However, these values were found by assuming that the optical constants of isolated PAHs are similar to those comprising the mantle and by ignoring impurities that might alter the PAH optical properties. Another drawback is that neutral PAHs should have absorption features in the UV that are not seen (Clayton et al. 2003), although Joblin et al. (1992) showed that this could be masked by averaging over a distribution of PAHs of different sizes. Also, it is unlikely that many PAHs are neutral in the diffuse ISM (e.g., LePage et al. 2003).

3.3. *Deviations from CCM*

Adherence to the R_V-dependent extinction law of CCM in our sample was also examined. In order to do this, we found the CCM curve that best fitted each extinction curve. The extinction curves were fitted with a CCM curve using a standard IDL curve fitting routine that minimized the χ^2. The values of R_V found this way were compared to those calculated using IR photometry, as shown in Figure 9. While there is some scatter, there is generally good agreement between the two values, with the fitted R_V being within 3 σ of the calculated value for 93% of

the sample. This indicates that the vast majority of sight lines agree with CCM within the measurement uncertainties. The near absence of non-CCM sight lines in the Galaxy could be attributed to the *IUE* data set somehow favoring lines of sight through CCM-type dust environments. *IUE* was a small telescope with limited dynamic range. As a result, there is little information on grain parameters deep inside dark clouds. The dust columns sampled in this study all have $A_V < 5$ mag.

Next we measured deviations of each measured extinction curve from its best-fit CCM curve. We followed the method of Mathis & Cardelli (1992, hereafter MC92), in which the authors specified the deviation at various wavelengths to be

$$\delta(x_i) = (A_\lambda / A_V)_i - (A_\lambda / A_V)_{\mathrm{CCM}}.$$

Plots of these deviations are shown in Figure 10 at 4.65, 4.90, 5.07, 5.24, and 7.82 μm^{-1}. The calculated and best-fit CCM extinction curves agreed within 2 σ of each other for all but four of the sight lines, HD 210121, HD 204827, HD 62542, and HD 29647, which are deviant at several wavelengths. Their deviations are shown in Table 7.

HD 204827 is an intriguing sight line. It has been shown that when a foreground reddening component has been removed, its extinction curve resembles that of the SMC, even though the environment of the dust in the HD 204827 cloud is quite different from that seen in the SMC sight lines (Valencic et al. 2003). A similar curve has been found toward HD 283809 (Whittet et al. 2004). The dust local to HD 204827 has high density. The HD 204827 dust cloud resembles a molecular cloud more than the diffuse ISM. The HD 204827 cloud is very rich in carbon molecules, showing large column densities of C_2, C_3, CH, and CN (Oka et al. 2003; Thorburn et al. 2003). The sight line to HD 204827 samples dust swept up by a supernova or hot star winds (Patel et al. 1998). In these respects, the
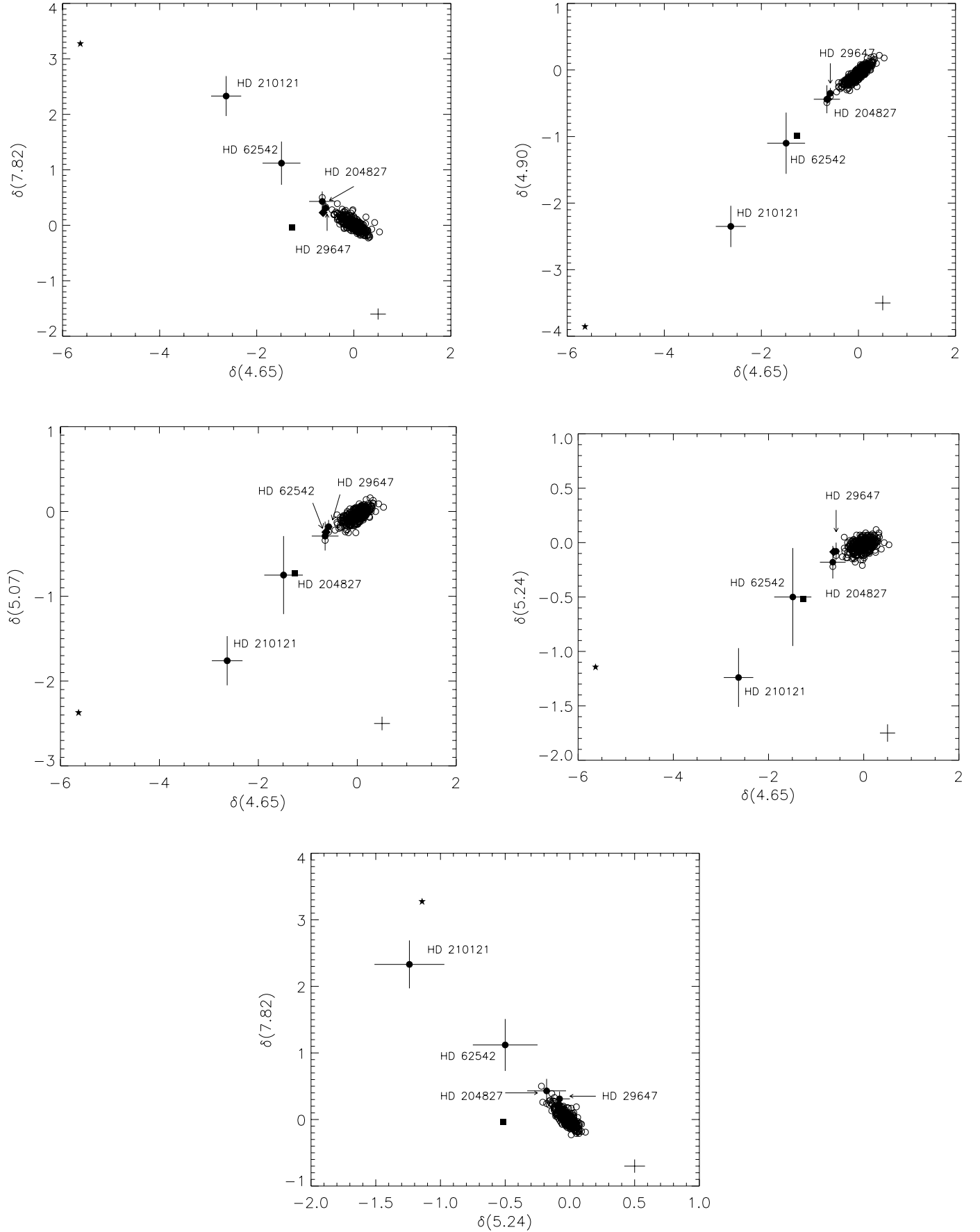
FIG. 10.—Deviations from R_V law at various wavelengths. Representative error bars are indicated. Four Galactic lines of sight with unusual extinction are named. The SD region average sight line (Clayton et al. 2000; *filled square*), average LMC (*filled triangle*), LMC2 Supershell (*filled diamond*), and SMC (*filled star*) are also plotted.

TABLE 7
DEVIATIONS OF NON-CCM SIGHT LINES

HD	$\delta(4.65)$	$\delta(4.90)$	$\delta(5.07)$	$\delta(5.24)$	$\delta(7.82)$
29647.......	−0.58	−0.35	−0.18	−0.08	0.31
62542........	−1.49	−1.10	−0.75	−0.50	1.12
204827......	−0.65	−0.44	−0.29	−0.18	0.43
210121......	−2.63	−2.35	−1.76	−1.24	2.33

HD 204827 dust is quite similar to the sight line toward HD 62542 (Cardelli & Savage 1988). Its dust is also rich in carbon molecules. The sight line to HD 62542 also lies on the edge of material swept up by a stellar wind bubble. The other two non-CCM, weak-bump, steep far-UV sight lines in the Galaxy, HD 29647, and HD 210121, are also associated with dense clouds (Cardelli & Savage 1988; Larson et al. 1996; Cardelli & Wallerstein 1989). The dust in the molecular cloud associated with HD 210121 is likely to have been processed as it was propelled into the halo during a Galactic fountain or other event. The final sight line, toward HD 29647, is sampling dust in a quiescent dense cloud. The steep far-UV extinction in these clouds helps shield the molecules in these clouds from dissociating UV radiation leading to larger column densities (Mathis 1990).

Figure 11 shows the deviations, $\delta(7.82)$ and $\delta(4.65)$, plotted against the column density of CN along the sight line divided by A_V for 46 sight lines from our sample, including the four non-CCM sight lines discussed above (Federman et al. 1994; Oka et al. 2003). CN can be used as an indicator of relatively dense regions in diffuse, molecule-rich clouds (Joseph et al. 1986; Gredel et al. 2002). The average $\delta(7.82)$ and $N(CN)/A_V$ (10^{13} cm^{-2} mag^{-1}) for the 42 CCM-like sight lines were 0.03 ± 0.03 and 0.33 ± 0.01, respectively. For the four non-CCM sight lines, these values were 1.06 ± 0.15 and 2.75 ± 0.15. These four sight lines have both high $N(CN)/A_V$ and significant deviation from CCM at $x = 7.82$ compared to the CCM-like sample. Similarly, Burgh et al. (2000) showed that sight lines with steep FUV rises tend to have high $N(CO)/E(B − V)$, although they did not notice any correlating weakness in the bump strength.

Virtually all of the non-CCM sight lines known today are in the (diffuse) Magellanic Clouds, not in dense Galactic clouds

(e.g., Gordon et al. 2003). Clayton et al. (2000) found that the average of seven low-density, low-reddening sight lines showed an extinction curve very similar to the LMC. These seven stars were found to be behind gas that showed signs of being subjected to shocks. The deviations from CCM for the average of these seven sight lines, as well as for the SMC and LMC average curves, were also found and are included in Figures 9 and 10. Similar deviations from CCM may arise in various dust environments.

3.4. The Updated CCM Law

The new extinction curves and values of R_V allow us to revise the CCM law. This was done by following the method described in CCM, that is, by plotting A_λ/A_V against R_V^{-1} for all wavelengths, then performing a linear least-squares fit of the resulting correlation. Thus, for all wavelengths, the extinction $A_\lambda/A_V = a(x) + b(x)/R_V$. Then $a(x)$ and $b(x)$ were plotted against x and fitted with a polynomial expression by minimizing χ^2. It was found that for 3.3 μm$^{-1} \geq x \geq 8.0$ μm^{-1},

$$a(x) = 1.808 - 0.215x - \frac{0.134}{(x - 4.558)^2 + 0.566} + F_a(x),$$

$$b(x) = -2.350 + 1.403x + \frac{1.103}{(x - 4.587)^2 + 0.263} + F_b(x),$$

where, for $x < 5.9$ μm^{-1},

$$F_a(x) = F_b(x) = 0.0,$$

and for 5.9 μm$^{-1} \leq x \leq 8.0$ μm^{-1},

$$F_a(x) = -0.0077(x - 5.9)^2 - 0.0003(x - 5.9)^3,$$
$$F_b(x) = 0.2060(x - 5.9)^2 - 0.0550(x - 5.9)^3.$$

A comparison of extinction laws is plotted in Figure 12. The most noticeable difference between the law found here and the original CCM law, the increase in the zero point of the UV extinction, is a consequence of the slightly higher value of the first term in $a(x)$. In 1988, CCM also found a higher value for this term (1.802) than in 1989 (1.752), when they found
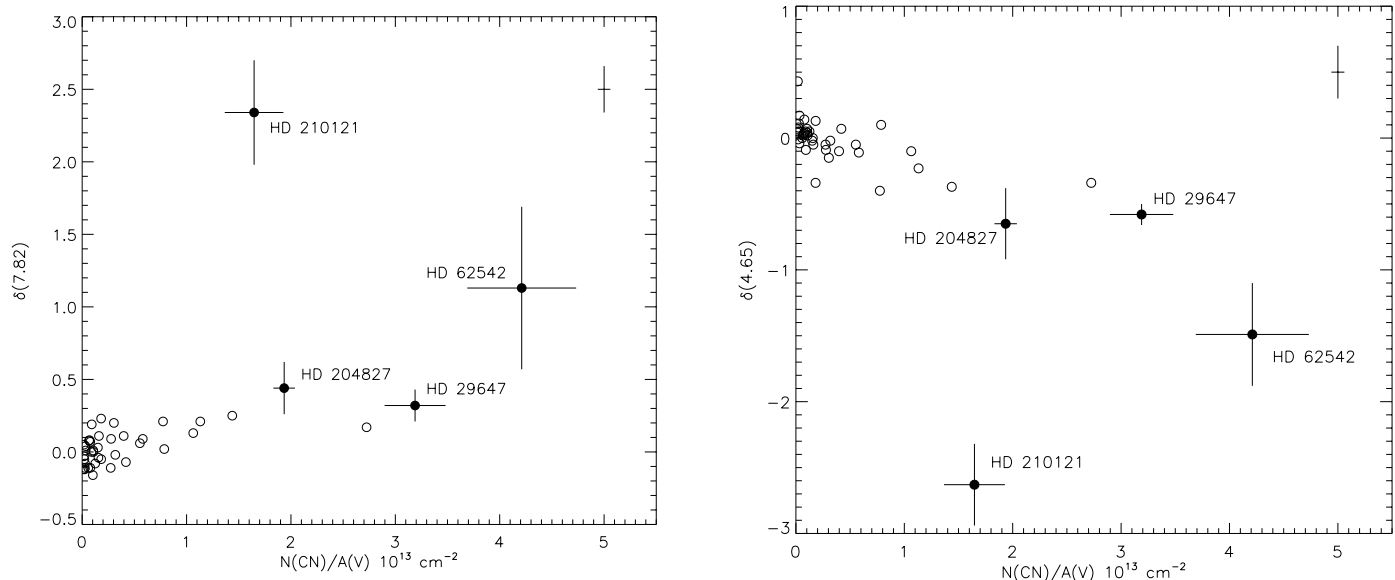

FIG. 11.—Deviation at 7.82 and 4.65 μm^{-1} vs. abundance of CN. Values of $N(CN)$ are from Federman et al. (1994) and Oka et al. (2003). Unusual Galactic sight lines are indicated with filled circles.
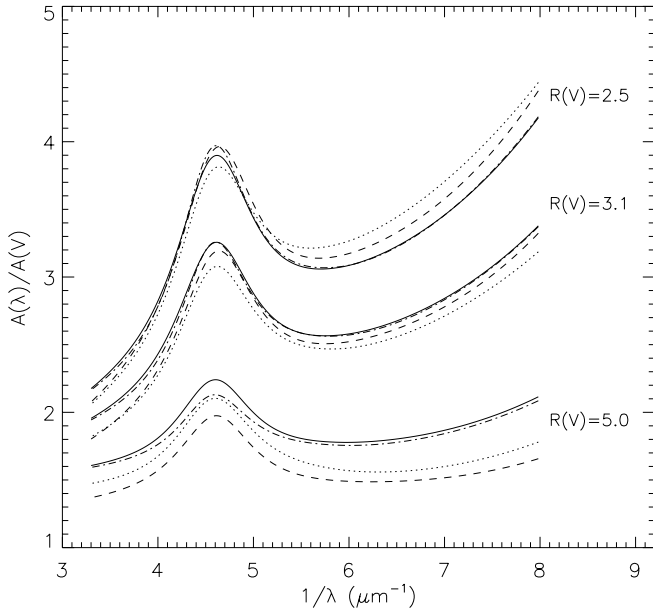
Fig. 12.—Comparison of extinction laws. *Solid line*: The extinction law derived in this work; *dashed line*: the original CCM law; *dash-dotted line*: the curve constructed with the FM parameter averages found in this work; *dotted line*: the curve constructed with the FM parameters suggested by Fitzpatrick (1999).

that the lower value, which was within the dispersion in the data, was needed for the curve to smoothly join the optical extinction data. Figure 12 also shows the resulting curve when the average FM parameter values are used to construct extinction curves at different values of R_V, in a fashion similar to that of Fitzpatrick (1999). The two methods of curve construction yield curves that are within 5% of each other for $2.5 \le R_V \le 5.0$ over the entire wavelength range. For all values of R_V, the difference is primarily in the bump height, or the FM parameter c_3. This is most noticeable for $5.0 < R_V \le 6.0$; here the curves agree to within 7%, with the curve found through the average FM parameters having a weaker bump than that predicted by either the revised or original CCM law. This can also be seen to a certain extent in Figure 4. A weakened bump at high R_V may be expected from the work of Whittet et al. (2004), which suggests that the bump carrier may be destroyed in dark clouds. Both the revised CCM curves and the average FM curves are within about 5% of the original CCM law for $2.5 \le R_V \le 3.5$. However, for increasing values of R_V, the difference between the curves increases as well, reaching 20% at $R_V \sim 5.0$. That the original CCM law agreed so well with the extinction curves examined here is an indicator of the sizes of the uncertainties on the data. Changes in the value of the extinction zero point is an important factor. If the first term in $a(x)$ is decreased by 0.20, the new CCM law and the original curve agree to within 15% for $2.5 \le R_V \le 6.0$ for $x < 7.0$ μm^{-1}, and within about 20% for $x \ge 7.4$ μm^{-1}. The dotted curve, constructed from Fitzpatrick (1999) suggested values of FM parameters with only c_2 (and through it, c_1) dependent on R_V, illustrates further the dependence of some FM parameters on R_V.

4. CONCLUSIONS

We have constructed a homogeneous database of UV extinction curves, all of which have been fitted by the FM relation

and for which values of R_V have been calculated. All extinction curves and FM parameters have been normalized to A_V rather than $E(B - V)$, so that relationships between parameters can be more easily seen. This is the largest and most comprehensive database of extinction curves yet constructed, sampling a wide variety of environments. It contains much longer sight lines than those included in previous studies (30 sight lines have $d > 5$ kpc), thus greatly increasing the volume of the Galaxy sampled compared to previous works. Over 150 sight lines have $d > 2$ kpc, so the regions of the Galaxy beyond the solar neighborhood are well represented.

The main results of this study are as follows:

1. The CCM extinction relation accurately describes the diffuse Galactic ISM in virtually all cases. Out of 417 sight lines, only four deviated consistently from their CCM extinction curves by more than 3 σ. This indicates that the physical processes that give rise to grain populations that have CCM-like extinction dominate the ISM, and thus, the quantity R_V can accurately describe the UV extinction for most sight lines. This implies that the grain populations responsible for different components of the extinction curve are being processed efficiently and systematically along most sight lines.

The new curves and R_V values allow for an updated CCM law to be made. The original and updated versions are within 5% of each other for $2.5 \le R_V \le 3.5$ over the full wavelength range covered, 3.3 $\mu m^{-1} \le x \le 8.0$ μm^{-1}. At higher values of R_V, the differences in the extinction zero point reduce the agreement in the curves to about 20%.

2. The bump width has a strong environmental dependence, with narrow bumps favoring diffuse sight lines and broad bumps favoring dense sight lines. Very broad bumps are rare, as only 21 out of 417 sight lines had $\gamma > 1.1$.

3. The central wavelength of the bump is invariant and can be regarded as a constant, with $x_0 = 4.59 \pm 0.01$. Unlike the other parts of the UV extinction curve, this parameter does not respond to different environments. The invariance of x_0, along with the observed variations in γ, puts strong constraints on possible bump-grain and mantle materials.

4. While there is evidence for shock processing in three of the four non-CCM sight lines, the common denominator is that all four sight lines have dense, molecule-rich clouds. They also have weak bumps and strong FUV extinction for their measured R_V CCM curves, especially those that pass through cold, quiescent regions. The weakened bump may reflect processing that modifies or destroys the bump carrier in dark clouds (Whittet et al. 2004). This is seen in the bumpless dust toward HD 204827 and HD 283809. Other dense sight lines with strong FUV extinction, HD 204827, HD 62542, and HD 210121, pass through dense clouds that may have been exposed to shocks or strong UV radiation that disrupt large grains, possibly resulting in a size distribution that is skewed toward small grains.

Together, the sight lines in the Galaxy and the Magellanic Clouds suggest that similar extinction properties may arise from very different environments.

REFERENCES

Aiello, S., Barsella, B., Chlewicki, G., Greenberg, J. M., Patriarchi, P., & Perinotto, M. 1988, A&AS, 73, 195
Aiello, S., Guidi, I., Barsella, B., Penco, U., & Perinotto, M. 1982, Ap&SS, 87, 463
Barbaro, G., Mazzei, P., Morbidelli, L., Patriarchi, P., & Perinotto, M. 2001, A&A, 365, 157
Bianchi, L., Clayton, G. C., Bohlin, R. C., Hutchings, J. B., & Massey, P. 1996, ApJ, 471, 203
Bless, R. C., & Savage, B. D. 1970, in IAU Symp. 36, Ultraviolet Stellar Spectra and Related Ground-based Observations, ed. L. Houziaux & H. E. Butler (Dordecht: Reidel), 28
Bohlin, R. C., Savage, B. D., & Drake, J. F. 1978, ApJ, 224, 132
Bohren, C. F., & Huffman, D. R. 1983, Absorption and Scattering of Light by Small Particles (New York: Wiley)
Borgman, J., van Duinen, R. J., & Koornneef, J. 1975, A&A, 40, 461
Burgh, E. B., McCandliss, S. R., Andersson, B.-G., & Feldman, P. D. 2000, ApJ, 541, 250
Cardelli, J., & Clayton, G. 1991, AJ, 101, 1021
Cardelli, J., Clayton, G., & Mathis, J. 1988, ApJ, 329, L33
———. 1989, ApJ, 345, 245
Cardelli, J., & Savage, B. 1988, ApJ, 325, 864
Cardelli, J., Sembach, K. R., & Mathis, J. S. 1992, AJ, 104, 1916
Cardelli, J., & Wallerstein, G. 1989, AJ, 97, 1099
Carnochan, D. J. 1986, MNRAS, 219, 903
Clayton, G. C., & Fitzpatrick, E. L. 1987, AJ, 93, 157
Clayton, G. C., Gordon, K. D., & Wolff, M. J. 2000, ApJS, 129, 147
Clayton, G. C., & Martin, P. G. 1985, ApJ, 288, 558
Clayton, G. C., et al. 1996, ApJ, 460, 313
———. 2003, ApJ, 592, 947
Cox, A. N., ed. 2000, Allen's Astrophysical Quantities (4th ed.; London: AIP)
Cutri, R. M., et al. 2003, 2MASS Second Incremental All Sky Point Source Catalog (Pasadena: IPAC)
Federman, S. R., Strom, C. J., Lambert, D. L., Cardelli, J. A., Smith, V. V., & Joseph, C. L. 1994, ApJ, 424, 772
Fitzpatrick, E. L. 1985, ApJS, 59, 77
———. 1986, AJ, 92, 1068
———. 1999, PASP, 111, 63
Fitzpatrick, E., & Massa, D. 1986, ApJ, 307, 286 (FM86)
———. 1988, ApJ, 328, 934 (FM88)
———. 1990, ApJS, 72, 163 (FM90)
Goebel, J. H. 1983, ApJ, 268, L41
Gordon, K., & Clayton, G. 1998, ApJ, 500, 816
Gordon, K., Clayton, G., Misselt, K., Landolt, A., & Wolff, M. 2003, ApJ, 594, 279
Gredel, R., Pineau des Forets, G., & Federman, S. R. 2002, A&A, 389, 933
Guetter, H. 1974, PASP, 86, 795
Haupt, H., & Schroll, A. 1974, A&AS, 15, 311
Hecht, J. 1986, ApJ, 305, 817

Hiltner, W. A. 1956, ApJS, 2, 389
Hiltner, W. A., & Johnson, H. L. 1956, ApJ, 124, 367
Jenniskens, P., & Greenberg, J. M. 1993, A&A, 274, 439
Joblin, C., Léger, A., & Martin, P. G. 1992, ApJ, 393, L79
Joseph, C. L., Snow, T. P., Jr., Seab, C., & Crutcher, R. M. 1986, ApJ, 309, 771
Kester, D. 1981, A&A, 99, 375
Koornneef, J. 1978, A&A, 68, 139
Koornneef, J., & Code, A. D. 1981, ApJ, 247, 860
Larson, K. A., Whittet, D. C. B., & Hough, J. H. 1996, ApJ, 472, 755
Le Page, V., Snow, T., & Bierbaum, V. 2003, ApJ, 584, 316
Luck, R. E., & Lambert, D. L. 1992, ApJS, 79, 303
Massa, D., & Fitzpatrick, E. L. 2000, ApJS, 126, 517
Massa, D., & Savage, B. D. 1984, ApJ, 279, 310
Massa, D., Savage, B. D., & Fitzpatrick, E. L. 1983, ApJ, 266, 662
Mathis, J. 1990, ARA&A, 28, 37
———. 1994, ApJ, 422, 176
Mathis, J., & Cardelli, J. 1992, ApJ, 398, 610
Meyer, D. M., & Savage, B. D. 1981, ApJ, 248, 545
Misselt, K., Clayton, G., & Gordon, K. 1999, ApJ, 515, 128
Naiman, A., Rosenfeld, R., & Zirkel, G. 1983, Understanding Statistics (3rd ed.; New York: McGraw-Hill)
Nandy, K., Morgan, D. H., Willis, A. J., Wilson, R., & Gondhalekar, P. M. 1981, MNRAS, 196, 955
Nandy, K., Thompson, G. I., Jamar, C., Monfils, A., & Wilson, R. 1975, A&A, 44, 195
———. 1976, A&A, 51, 63
Nichols, J. S., & Linsky, J. L. 1996, AJ, 111, 517
Nicolet, B. 1978, A&AS, 34, 1
Oka, T., Thorburn, J. A., McCall, B. J., Friedman, S. D., Hobbs, L. M., Sonnentrucker, P., Welty, D. E., & York, D. G. 2003, ApJ, 582, 823
Papaj, J., & Krelowski, J. 1992, Acta Astron., 42, 211
Papaj, J., Krelowski, J., & Wegner, W. 1991, MNRAS, 252, 403
Patel, N. A., Goldsmith, P. F., Heyer, M. H., Snell, R. L., & Pratap, P. 1998, ApJ, 507, 241
Savage, B. D., Massa, D., Meade, M., & Wesselius, P. R. 1985, ApJS, 59, 397
Schild, R., Garrison, R., & Hiltner, W. 1983, ApJS, 51, 321
Seaton, M. J. 1979, MNRAS, 187, P73
Snow, T. P., Jr., & Seab, C. G. 1980, ApJ, 242, L83
Sorrell, W. H. 1990, MNRAS, 243, 570
Thorburn, J. A., et al. 2003, ApJ, 584, 339
Valencic, L. A., Clayton, G. C., Gordon, K. D., & Smith, T. L. 2003, ApJ, 598, 369
Vallée, J. P. 2002, ApJ, 566, 261
Warren, S. G. 1984, Appl. Opt., 23, 1206
Whittet, D., Senoy, S., Clayton, G., & Gordon, K. 2004, ApJ, 602, 291
York, D. G., Drake, J. F., Jenkins, E. B., Morton, D. C., Rogerson, J. B., & Spitzer, L. 1973, ApJ, 182, L1

ERRATUM: "ULTRAVIOLET EXTINCTION PROPERTIES IN THE MILKY WAY" (2004, ApJ, 616, 912)

Lynne A. Valencic[1,3], Geoffrey C. Clayton[1], and Karl D. Gordon[2]
[1] Department of Physics and Astronomy, Louisiana State University, Baton Rouge, LA 70803, USA
[2] Steward Observatory, University of Arizona, Tucson, AZ 85721, USA
Received 2014 August 4; published 2014 September 5

In the published version of this paper, there were typographical errors in Section 3.4, in the updated CCM law's description of the far-UV extinction. They do not effect the results of the study, as the correct values were used in the analysis, but they may lead to errors if used in future works. The corrected equations are below.

For $5.9\,\mu\mathrm{m}^{-1} \leqslant x \leqslant 8.0\,\mu\mathrm{m}^{-1}$,

$$F_a(x) = -0.0077(x - 5.9)^2 - 0.0030(x - 5.9)^3$$

and

$$F_b(x) = 0.2060(x - 5.9)^2 + 0.0550(x - 5.9)^3.$$

---

[3] Currently at Instituto de Astronomi, UNAM, Apartado Postal 877, Ensenada, Baja California 22800, Mexico.